

Performance of a Bender for a Water-cooled Monochromator Crystal at a High Power Wiggler Beamline of the ESRF

Hitoshi Yamaoka¹⁾, Andreas K. Freund²⁾, Kiyotaka Ohtomo¹⁾ and Michael Krumrey²⁾

1) SPring-8, Kamigori, Ako-gun, Hyogo 678-12, Japan

2) European Synchrotron Radiation Facility, BP-220, F 38043, Grenoble Cedex, France

Large heat loads from synchrotron radiation insertion device beamlines induce surface slope errors like thermal bumps, thermal bowing as well as lattice constant variations on monochromator crystals[1]. As normal water cooling is no longer sufficient at the extremely high heat loads of third generation facilities, cooling with micro-channel, gallium cooling, liquid nitrogen cooling or water jet cooling have been proposed to preserve the source brightness. Another solution consists of active compensation of the deformation under heat load. This requires a bender mechanism, it can also be used to correct a possible intrinsic curvature. In high heat load beamlines that commonly use cooled crystals, it is difficult to combine both systems of water cooling and bender. In this study the performance of the system that is compatible with a directly water cooled crystal was tested at the material science beamline (BL2) of the ESRF[2-4].

A schematic view of the bender with the water cooled Si crystal is shown in Fig. 1.

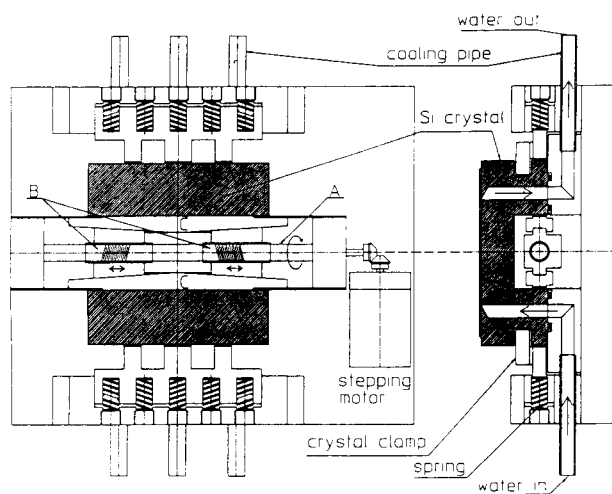


Fig. 1 Top view and cross section of the crystal bender with Si crystal. The thin Si wafer is bonded to the grooved Si substrate. Rotation of the center screw A leads the linear movement of the part B relative to the wedge guides C. When both parts B are moved inwards the crystal legs move outwards.

The beam direction is parallel to the cooling channels. The crystal expander is inside of a wide channel grooved into the substrate crystal. The crystal bending is achieved by pushing the channel walls. Rotation of the center screw A leads the linear movement of the part B relative to the wedge guides C. When both parts B are moved inwards the crystal legs move outwards. The crystal is pushed back by hard springs from both end sides if the part B is moved outwards. The center screw A can be rotated by a remote control system using a stepper motor. Step size and total stroke of the motor are 0.05 μm and a few tens of μm , respectively. The force is applied through 5 springs with a spring constant $1.33 \times 10^4 \text{ N/m}$. A 1/50 worm gear is placed between the motor and the screw A. The motor torque is 0.13 Nm. A special plastic material, turcite B, is inserted to reduce the friction between metal parts.

Three dimensional finite element analysis was performed to calculate the deformation for different forces using the ANSYS code. A half model is assumed for the analysis using a Young modulus of $1.1 \times 10^{11} \text{ Pa}$, density of $2.34 \times 10^3 \text{ kg/m}^3$ and Poisson ration of 0.281. We get a nearly ideal cylindrical curvature to within $\pm 20 \text{ mm}$ from the center, becoming almost linear towards the edges of the crystal. In the experiment the maximum beam foot print along the beam direction on the crystal surface is $\pm 17 \text{ mm}$ which is the inner part of the calculated curve.

The beam profile was measured by Be wire monitors. The beam footprint on the crystal surface was 34 mm long and 78 mm wide with a 20.3 mm wiggler gap. It was only 13 mm wide at 80 mm gap due to the limited horizontal divergence. The incident total power at a 80 mm gap was about 6 W and the beam was then considered as "cold beam" without thermal deformations. Figure 2 shows an example of the heat load effect on the change in the Si (111) rocking curve width for the bent crystal at two different wiggler gaps. Pure heat load effect on the increase of the rocking curve width was 1.5 arc seconds for incident total power of 1440 W and power density of 0.54 W/mm^2 at 72 mA stored current. After

deconvolution with the theoretical 6 arc seconds width and assuming Gaussian rocking curve profiles, the pure thermal strain was about 5 arc seconds. The effect of the beam induced thermal strain of 1.5 arc seconds width under 1440 W input power for the bent crystal was almost the same as the unbent crystal of 1.1 arc seconds under 840 W power.

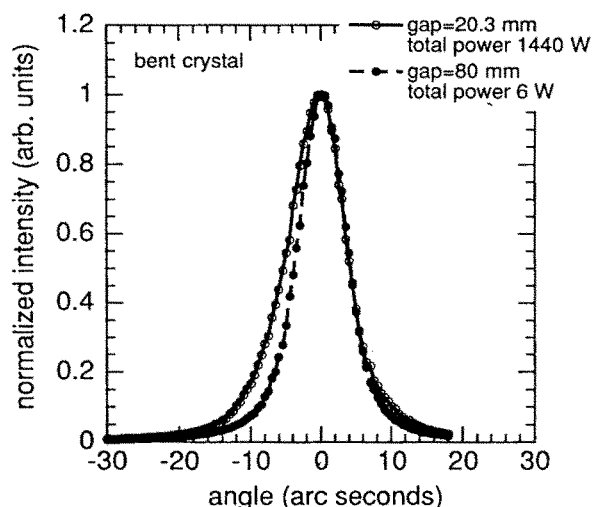


Fig. 2 Heat load effect on the Si (111) rocking curve at 13 keV for a bent crystal. At 1440 W the width increases to 9.5 arc seconds, compared to 8 arc seconds at 6 W.

Figure 3 shows a typical example of the bend effect under high heat load condition. At an optimum force the intrinsic surface curvature and the power induced deformation were compensated and the width of the rocking curve could be decreased from 17 arc seconds to 9.5 arc seconds. Thus for an incident total power of 1440 W and a power density of 0.54 W/mm² only a broadening of 1.5 arc seconds remained compared to the cold beam rocking curve shown in Fig. 2. On further increase of the bending force, the rocking curve width started to increase again. After deconvolution with a heat load component of about 5 arc seconds and theoretical value of 6 arc seconds for the experimental value of 9.5 arc seconds, a remaining uncompensated component due to bending or bonding strain was about 5.2 arc seconds.

A bender developed for a water cooled monochromator has been tested at the materials science wiggler beamline of the ESRF. The synchrotron radiation beam exposed the monochromator crystal to almost 1.5 kW. The beam-induced broadening of the rocking curve as well as the intrinsic curvature could be compensated by the bender to within 1.5 arc seconds. The remaining broadening was due to residual bonding or bending

strain of the wafer. The bender will be well suited for compensating the slope error induced by larger heat loads or to focus the beam vertically.

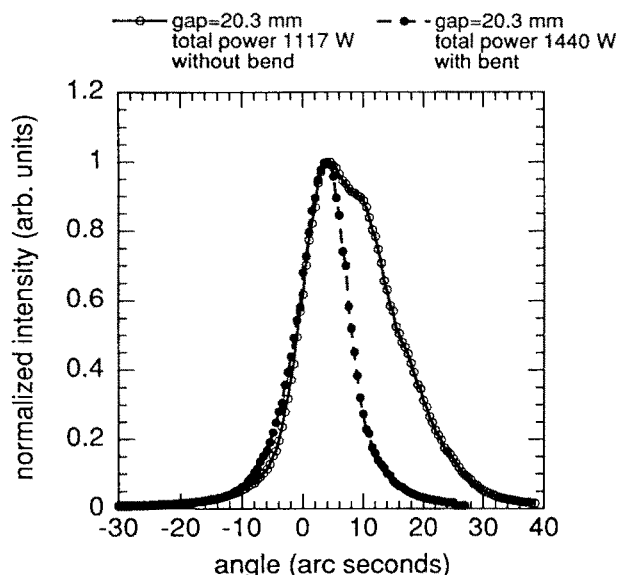


Fig. 3 Bending effect on the Si (111) rocking curve. A wiggler gap, total power and beam footprint were 20.3 mm, 1440 W (1117 W for the measurement of the unbent crystal), and 34x78 mm², respectively, on the crystal surface. The width decreases from 17 to 9.5 arc seconds.

References

- [1] H. Yamaoka, X. M. Tong, T. Uruga and Y. Sakurai, Proc. Soc. Photo-Opt. Instrum. Eng. **1739**, 522 (1992).
- [2] H. Yamaoka, A. K. Freund, K. Ohtomo and M. Krumrey, Rev. Sci. Instrum. **66** 2092 (1995).
- [3] H. Yamaoka, D. Häusermann, A. K. Freund and M. Krumrey, Nucl. Instrum. & Method **A351**, 559 (1994).
- [4] Å. Kvik and M. Wulff, Rev. Sci. Instrum. **63**, 1073 (1992).